

8873

NACA TN 2483

0065582



NATIONAL ADVISORY COMMITTEE FOR AERONAUTICS

TECHNICAL NOTE 2483

EFFECT OF FUSELAGE AND TAIL SURFACES ON LOW-SPEED YAWING
CHARACTERISTICS OF A SWEEP-WING MODEL AS DETERMINED
IN CURVED-FLOW TEST SECTION OF LANGLEY
STABILITY TUNNEL

By John D. Bird, Byron M. Jaquet, and John W. Cowan

Langley Aeronautical Laboratory
Langley Field, Va.



Washington
October 1951

AFMDC
TECHNICAL LIBRARY
AFL 2811

1
NATIONAL ADVISORY COMMITTEE FOR AERONAUTICS

TECHNICAL NOTE 2483

EFFECT OF FUSELAGE AND TAIL SURFACES ON LOW-SPEED YAWING

CHARACTERISTICS OF A SWEEP-WING MODEL AS DETERMINED

IN CURVED-FLOW TEST SECTION OF LANGLEY

STABILITY TUNNEL¹

By John D. Bird, Byron M. Jaquet, and John W. Cowan

SUMMARY

A wind-tunnel investigation was made in the Langley stability tunnel for determining the influence of the fuselage and tail surfaces on the rotary derivatives in yawing flight of a transonic airplane configuration which had the wing and tail surfaces swept back 45° . The results of the determination of the rate of change of the yawing-moment coefficient with yawing velocity by two oscillation techniques agreed well with the determinations by the curved-flow procedure. The vertical tail was the main contributor to this derivative. The value for the complete model was essentially constant up to the angle of attack corresponding to maximum lift coefficient and could be accurately calculated when proper account was taken of the end-plate effect of the horizontal tail on the vertical tail. The rate of change of rolling-moment coefficient with yawing velocity was mainly a contribution of the wing. This derivative increases approximately linearly with angle of attack to the angle of attack where the curves of lift and pitching-moment coefficient plotted against angle of attack develop nonlinearities.

INTRODUCTION

Results are presented of one of a series of tests made to investigate the factors affecting the rotary derivatives of various swept-wing configurations. This investigation was begun because conventional straight-flow tests of swept wings had given results that were very different, particularly at moderate and high lift coefficients, from those generally obtained from tests of unswept wings and that were of a nature not readily adaptable to thorough mathematical analysis.

¹Supersedes the recently declassified RM 18G13, "Effect of Fuselage and Tail Surfaces on Low-Speed Yawing Characteristics of a Swept-Wing Model as Determined in Curved-Flow Test Section of Langley Stability Tunnel" by John D. Bird, Byron M. Jaquet, and John W. Cowan, 1948.

The investigation discussed herein was conducted for determination of the influence of the tail surfaces and the fuselage on the low-speed yawing derivatives of a transonic airplane configuration having the wing and tail surfaces swept back 45° .

These tests were conducted in the 6- by 6-foot curved-flow test section of the Langley stability tunnel which was designed for simulation of steady yawing or pitching flight of the rigidly mounted model. The principle of operation of this test section was conceived by Mr. M. J. Bamber while he was a member of the staff of the Langley Laboratory.

SYMBOLS

The results of the tests are presented as standard coefficients of forces and moments which are referred to stability axes for which the origin is assumed to be at the projection on the plane of symmetry of the quarter-chord point of the mean geometric chord of the wing of the model.

The stability-axis system is shown in figure 1. The coefficients and symbols used herein are defined as follows:

C_L	lift coefficient $\left(\frac{\text{Lift}}{qS}\right)$
C_D	drag coefficient $\left(\frac{-X}{qS} \text{ at } \psi = 0^\circ\right)$
C_Y	lateral-force coefficient $\left(\frac{Y}{qS}\right)$
C_m	pitching-moment coefficient $\left(\frac{M}{qS\bar{c}}\right)$
C_n	yawing-moment coefficient $\left(\frac{N}{qSb}\right)$
C_l	rolling-moment coefficient $\left(\frac{L}{qSb}\right)$
X	longitudinal force
Y	lateral force

M	pitching moment about Y-axis
N	yawing moment about Z-axis
L	rolling moment about X-axis
R	Reynolds number
q	dynamic pressure $\left(\frac{1}{2}\rho V^2\right)$
ρ	mass density of air
V	free-stream velocity
S	wing area
\bar{c}	mean aerodynamic chord of wing
b	span of wing
σ	angle of air stream with respect to uncurved tunnel center line, positive when air is approaching from right facing upstream
α	angle of attack measured in plane of symmetry, degrees
β	angle of sideslip, degrees
ψ	angle of yaw, degrees
$\frac{rb}{2V}$	yawing-velocity parameter
r	angular velocity in yaw, radians/sec
$\dot{\beta}$	rate of change of angle of sideslip with time $\left(\frac{d\beta}{dt}\right)$

$$C_{Y_r} = \frac{\partial C_Y}{\partial \frac{rb}{2V}}$$

$$C_{l_r} = \frac{\partial C_l}{\partial \frac{rb}{2V}}$$

$$C_{n_r} = \frac{\partial C_n}{\partial \frac{rb}{2V}}$$

$$C_{n\beta} = \frac{\partial C_n}{\partial \frac{\beta b}{2V}}$$

$$C_{z\beta} = \frac{\partial C_z}{\partial \beta}$$

APPARATUS AND MODEL

The tests reported herein were run in the 6- by 6-foot test section of the Langley stability tunnel. This test section was designed for testing models in an air flow which simulates steady yawing or pitching flight. Simulation of a steady curved-flight condition in a wind tunnel where the model is fixed to the balance system necessitates reproduction of the relative motion existing between the airplane and air stream in curved flight. This result may be accomplished by obtaining an air flow which is curved in a circular path in the vicinity of the model and which has a velocity variation normal to the streamlines in direct proportion to the local radius of curvature of the flow. Such a flow is possible in the 6- by 6-foot test section of the Langley stability tunnel which is equipped with flexible side walls for curving the air stream and specially constructed drag screens for producing the desired velocity gradient in the jet. These screens are located at the upstream end of the test section. Each screen is composed of a wooden frame and vertical wires having a varying spacing across the jet. Screens are added for each increment of increase in flow curvature. Figure 2 is a photograph of a model mounted in the section for yawing tests. Figure 3 is a schematic diagram of the test section showing its component parts and the survey stations used for calibration purposes. The model may be mounted from the side wall for pitching tests as well as in the position shown.

A curved flow in the tunnel for simulation of a curved-flight condition of a given curvature has specific variations in the free stream of the dynamic, static, and total pressures normal to the streamlines. The variation of these pressures in the free stream along a streamline ahead of and behind the test region is zero. The velocity variation normal to the streamlines and thus the dynamic pressure is determined by the particular flight path being simulated. The static- and total-pressure variations may be obtained by equating the pressure forces in the air to the centrifugal forces. These factors, specifically the dynamic and total pressure together with the angularity of the air stream, were used during calibration of the test section to indicate how well the test section reproduced ideal conditions.

Representative surveys made at the center and rear survey stations for various flow curvatures are given in figure 4. This figure which presents the variation of dynamic pressure and air-stream angularity with distance across the tunnel indicates reasonably good agreement between the ideal and actual result for the model test region in the center of the tunnel. Large angles of yaw would place the tail surfaces of the model in a region where the flow representation is not so accurate as in the center region.

Curved flow is not an exact simulation of curved flight because of the static-pressure gradient which exists normal to the streamlines in curved flow. This gradient produces a buoyancy which does not exist in curved flight and, in addition, a tendency for the low-energy boundary-layer air of the model to flow toward the center of rotation. The normal curved-flight tendency is for the boundary layer to move outward. A correction has been devised to account for the effect of the buoyancy force. The boundary-layer effect is as yet considered to be second order.

In addition to the static-pressure gradient, there exists behind the drag screens a rather high degree of turbulence which is graded according to the spacing of the wires. The influence of the gradient in the turbulence on the aerodynamic characteristics of the model is believed to be small because the mixing of the turbulent wakes is believed to be sufficient to cause a relatively uniform turbulence downstream at the test section. The high turbulence, however, may well produce measurable effects on airfoils normally having extensive regions of laminar flow. These effects should be confined mainly to drag and maximum-lift characteristics and should not greatly affect the accuracy of determination of rotary derivatives if all tests used for such determinations are made under approximately the same turbulence conditions.

The model used for the tests was a transonic configuration having the wing (aspect ratio 2.61) and tail surfaces swept back 45° . These surfaces had NACA 0012 airfoil sections normal to the leading edge and a taper ratio of 1. The fuselage was a body of revolution which had a circular-arc profile and a fineness ratio of 8.34. Construction was of laminated mahogany with a waxed lacquer finish. A view of the model mounted in the tunnel is shown in figure 2, and pertinent geometric characteristics of the model are given in figure 5.

TESTS

The test configurations and the symbols used in identifying the data in the figures are given in the following table:

Wing	W
Fuselage	F
Wing and fuselage	W + F
Wing, fuselage, and vertical tail	W + F + V
Wing, fuselage, vertical tail, and horizontal tail	W + F + V + H

Curved-Flow Tests

The rolling moment, yawing moment, and lateral force were measured through the angle-of-attack range for all model configurations at yawing-flow curvatures corresponding to values of $\frac{rb}{2V}$ of 0, -0.032, -0.067, and -0.088. These data were used for determining the rotary derivatives C_{n_r} , C_{l_r} , and C_{Y_r} for the angle-of-attack range by plotting the coefficients against the flight-path curvature and determining the slope of the straight line most logically faired through the four test points.

Free-Oscillation Tests

Values of C_{n_r} were determined from free-oscillation tests for comparison with the curved-flow results. For these tests, the model was mounted in the tunnel with no constraint in yaw other than the aerodynamic forces and a spring of sufficient strength to make the variation of yawing moment N with angle of yaw ψ of the model-spring combination stable with the tunnel operating. The damping in yaw C_{n_r} was determined from the rate of decay of a free oscillation of the model in yaw. Details of this procedure are described in reference 1.

Forced-Oscillation Tests

Tests were run on the complete model by a forced-oscillation procedure in which continuous records were made of the angle of sideslip, yawing acceleration, and applied yawing moment necessary to maintain a steady oscillation of the model in yaw about a fixed axis when under the influence of the air stream. These records were analyzed by determining the forces acting on the model at the time that the acceleration was zero and solving for the damping derivative C_{n_r} . The data obtained by this procedure are not expected to be so accurate as those obtained by the free-oscillation technique because of the difficulty of obtaining records free of random disturbances. Each test point presented herein was obtained by averaging the results of a number of tests, and the data are believed to be accurate only to approximately 10 percent of its minimum value. However, this technique enabled determination of results

in the high angle-of-attack range where difficulty was experienced in obtaining reliable results by the free-oscillation technique. All tests were run at a dynamic pressure of 25 pounds per square foot, which corresponds to a Mach number of 0.13 and a Reynolds number of 1.07×10^6 .

CORRECTIONS

The following corrections for jet-boundary effects were applied to the data:

$$\alpha = \alpha_T + 0.83 C_{L_T}$$

$$C_D = C_{D_T} + 0.014 C_{L_T}^2$$

$$C_m = C_{m_T} - 0.00023 \alpha_T \text{ (complete model only)}$$

$$C_{l_r} = 0.980 C_{l_{rT}}$$

$$C_{n_r} = C_{n_{rT}} - 0.0185 C_{l_{rT}} C_{L_T} \text{ (vertical-tail configurations only)}$$

where the subscript T refers to uncorrected tunnel measurements.

The following correction, taken from an analysis made in the Langley stability tunnel, was applied to account for the effect of the lateral horizontal buoyancy on the lateral-force yawing rotary derivative:

$$C_{Y_r} = C_{Y_{rT}} - \frac{4v}{Sb} (1 + 2k_1 \cos^2 \alpha + 2k_3 \sin^2 \alpha)$$

where

- v volume of body
- k_1 additional-mass coefficient of body for translation along X-axis
- k_3 additional-mass coefficient of body for translation along Z-axis

No corrections were made for tunnel blocking or support-strut tares except for the case of the derivative C_{l_r} . In this case, the tare at zero angle of attack was applied to the data throughout the angle-of-attack range. This correction is believed to be sufficiently accurate because, although there are large tare corrections to the drag coefficient, the corrections to the derivatives of the forces and moments with respect to angular displacement or velocity are in most cases negligible.

RESULTS AND DISCUSSION

The lift, drag, and pitching-moment characteristics of the various model test configurations throughout the angle-of-attack range are presented in figure 6. These data were obtained from tests made in the 6-foot circular test section of the Langley stability tunnel at a Reynolds number of 1.40×10^6 and are included for the sake of logical completeness. Check tests at the Reynolds number of the present tests indicate that the difference in Reynolds number between the two tests has little effect on the aerodynamic coefficients of the model. The values of the derivative C_{n_r} obtained by the curved-flow and free-oscillation technique for the various model configurations are presented in figure 7. Data are also presented for the complete model as determined by the forced-oscillation technique previously described and for the complete model with and without horizontal tail as calculated for the effect of the vertical tail by the use of the end-plate data given in reference 2. The results indicate reasonably good agreement between the curved-flow, free-oscillation, and calculated vertical-tail results up to angles of attack of approximately 14° beyond which the variation of yawing-moment coefficient with angle of sideslip of the model becomes nonlinear. The agreement between the calculated and experimental result indicates that the derivative C_{n_r} of an airplane may be estimated very accurately for the angle-of-attack range where nonlinearities in the lift and pitching-moment characteristics do not exist merely by considering the effect of the vertical tail and the appropriate end-plate effect of the horizontal tail.

The nonlinear variation of yawing-moment coefficient with angle of sideslip mentioned makes the mathematical solution used in analyzing the results of the free-oscillation technique not strictly applicable, although the results may still be used as an indication of trends. Results for the complete model by the forced-oscillation technique described previously show higher damping at angles of attack beyond 14° than do those of the curved-flow procedure. A few exploratory free-oscillation tests made in the Langley stability tunnel have indicated a similar result for the wing alone with positive damping at an angle of attack of approximately 16° .

It must be realized that an exact check between oscillation tests and curved-flow results should not be expected, because the factor determined by the oscillation test is the sum of the effect of the derivatives C_{n_r} and C_{n_β} , the latter of which arises from additional-mass considerations. A constant value of r at zero sideslip implies a circular flight path to which the airplane is always tangent. A constant value of β , however, implies a constantly increasing sideslip. The oscillation test described herein represents a condition where $\dot{\beta}$ is always the negative of r .

Reference 3 considers C_{n_β} to be small compared with C_{n_r} . Calculations indicate that the effect of C_{n_β} of the vertical tail of the model (presumably the main contributor at low angles of attack) is of the same sign and approximately 10 percent of the value of C_{n_r} of the complete model. A large increase in the value of C_{n_β} of the wing at high angles of attack could easily account for the discrepancy between the curved-flow and oscillation tests. These differences may, however, be associated with aerodynamic lag effects and the cyclic nature of the motion.

A comparison of the values of C_{n_r} , C_{l_r} , and C_{Y_r} of the various model configurations throughout the angle-of-attack range as determined by the curved-flow procedure may be made from the data presented in figure 8. The value of C_{n_r} of the complete model is almost constant for angles of attack up to maximum lift and is primarily a function of the vertical tail. The effect of the vertical tail on this derivative may be accurately calculated as has been shown previously. Addition of the horizontal tail to the model increases C_{n_r} negatively in proportion to the end-plate effect on the vertical tail. Throughout the angle-of-attack range the wing alone has small values of C_{n_r} which are positive in the neighborhood of an angle of attack of 16° and for angles of attack above 22° . The values of C_{n_r} for the fuselage alone are zero up to an angle of attack of 12° but become positive for higher angles of attack.

A comparison of the values of $C_{\dot{\lambda}_r}$ for all model configurations tested indicates that this derivative is mainly a function of the characteristics of the wing, as might logically be expected (fig. 8). The derivative $C_{\dot{\lambda}_r}$ increases approximately linearly up to the angle of attack at which nonlinearities appear in the curves of lift and pitching-moment coefficients. Beyond this point $C_{\dot{\lambda}_r}$ tends to remain constant until a return to zero occurs at the angle of attack corresponding to maximum lift coefficient. Higher Reynolds numbers than that used for the present tests may tend to change the extent of the linear range of this curve. Tests made in the Langley 19-foot pressure tunnel at Reynolds numbers up to 8.0×10^6 have indicated such an effect for the derivative $C_{\dot{\lambda}_\beta}$. At higher angles of attack $C_{\dot{\lambda}_r}$ is, in general, negative. The vertical tail, although its effect is small, is second in importance to the wing as a contributor to $C_{\dot{\lambda}_r}$. This increment may be noted in figure 8 and is positive for the low angles of attack where the center of pressure of the vertical tail is above the X-axis and negative for the high angles of attack where the converse is true.

The values of the derivative $C_{\dot{Y}_r}$ are small and usually negative throughout the angle-of-attack range for the wing alone and for the model without the tail surfaces (fig. 8). The vertical tail contributes a positive increment to the value of $C_{\dot{Y}_r}$ which, even though its magnitude is small with regard to its effect on the dynamic equations, is the largest contributed by any component of the model. A slight negative increase of the derivative with angle of attack may be noted for all model configurations. The fuselage contributes a small negative amount to the value of $C_{\dot{Y}_r}$ except at very high angles of attack.

The results of the tests and calibrations in the curved-flow test section of the Langley stability tunnel indicate that this facility satisfactorily measures the rotary derivatives caused by yawing velocity. The technique may be equally well applied to determining the rotary derivatives caused by pitching velocity. These facts should make the curved-flow technique extremely valuable as a research tool.

CONCLUSIONS

An investigation of the effect of fuselage and tail surfaces on low-speed yawing characteristics of a swept-wing model as determined in the curved-flow test section of the Langley stability tunnel indicated the following conclusions:

1. Good agreement was obtained for measurement of the rate of change of yawing-moment coefficient with yawing velocity by the curved-flow and oscillation techniques employed in this investigation for angles of attack up to 14° . The ability of the curved-flow technique to measure all pertinent derivatives with respect to the flight-path curvature caused by yawing or pitching velocities should make this facility extremely valuable as a research tool.

2. The vertical tail was by far the main contributor to the value of the rate of change of yawing-moment coefficient with yawing velocity of the model. In general, sufficiently accurate estimates of this derivative could be made by accounting for the effect of the vertical tail including any end-plate effect contributed by the horizontal tail. The value of this derivative for the complete model was essentially constant for angles of attack up to maximum lift.

3. The rate of change of rolling-moment coefficient with yawing velocity was mainly a contribution of the wing and increased linearly with angle of attack to the point where nonlinearities in the curves of pitching moment and lift coefficient plotted against angle of attack became noticeable. Beyond this point the derivative had a tendency to remain constant until a return to zero occurred at the angle of attack corresponding to maximum lift coefficient.

4. The values of the rate of change of lateral-force coefficient with yawing velocity are small for all model test configurations for angles of attack up to maximum lift coefficient. The vertical tail is the largest contributor to this derivative.

Langley Aeronautical Laboratory
National Advisory Committee for Aeronautics
Langley Field, Va., April 13, 1948

REFERENCES

1. Campbell, John P., and Mathews, Ward O.: Experimental Determination of the Yawing Moment Due to Yawing Contributed by the Wing, Fuselage, and Vertical Tail of a Midwing Airplane Model. NACA ARR 3F28, 1943.
2. Murray, Harry E.: Wind-Tunnel Investigation of End-Plate Effects of Horizontal Tails on a Vertical Tail Compared with Available Theory. NACA TN 1050, 1946.
3. Simmons, L. F. G.: Note Relating to Two Oscillation Methods in Use for Determining Rotary Derivatives of Models. R. & M. No. 711, British A.R.C., 1921.

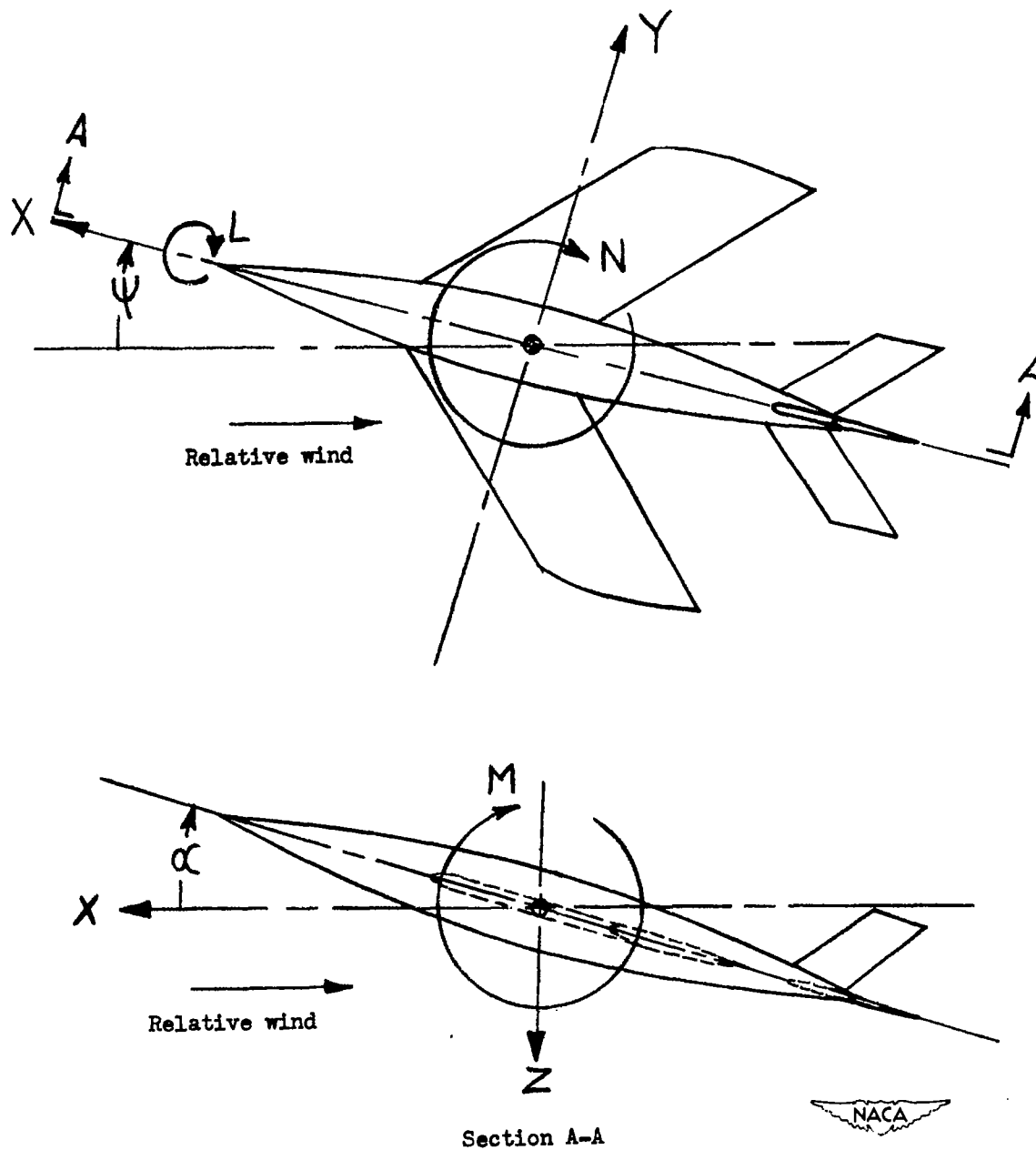


Figure 1.- Stability system of axes. Positive values of forces, moments, and angles are indicated by arrows.

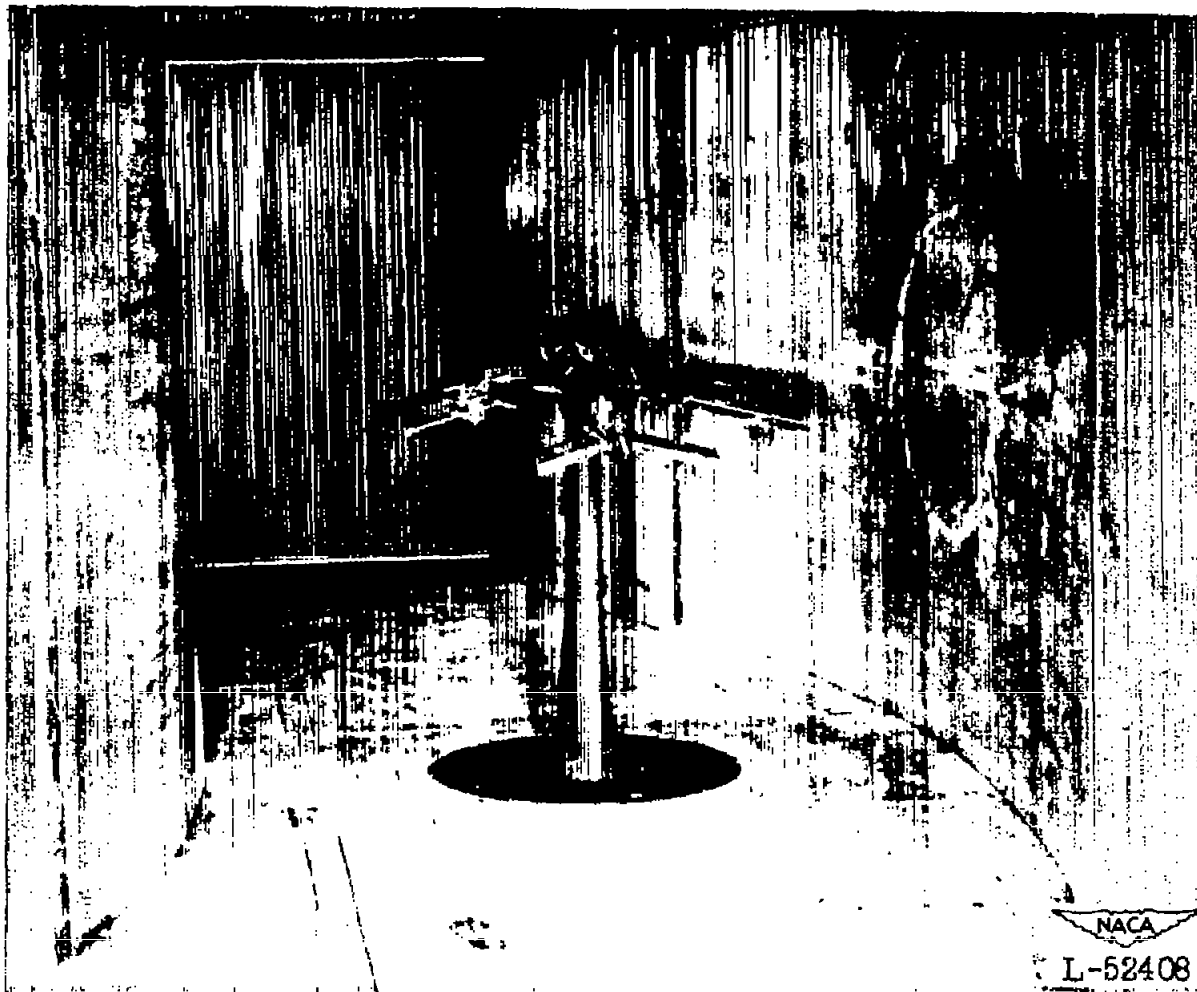


Figure 2.- Model mounted in curved-flow test section of the Langley stability tunnel.

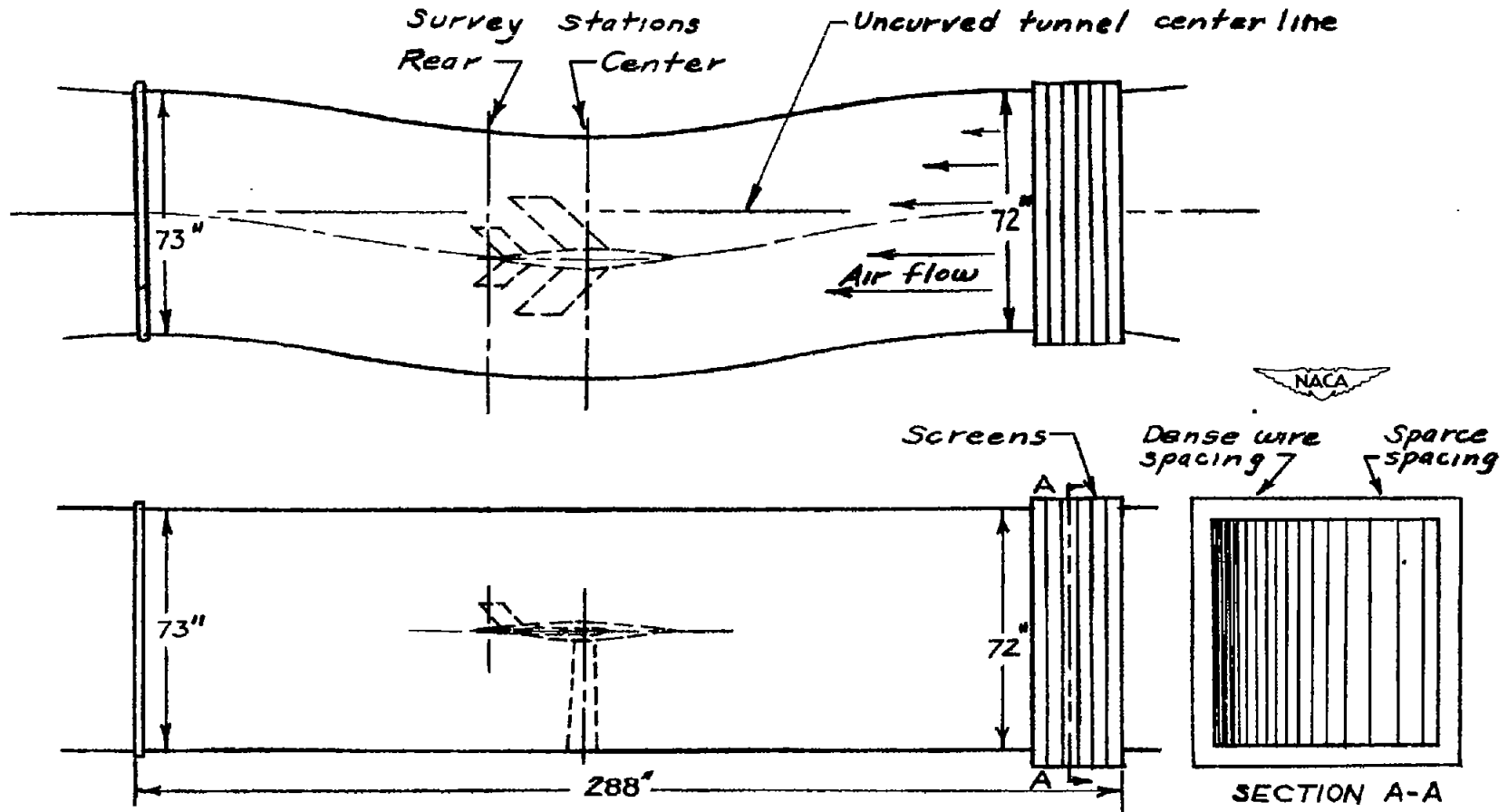


Figure 3.- Schematic diagram of curved-flow test section of the Langley stability tunnel.

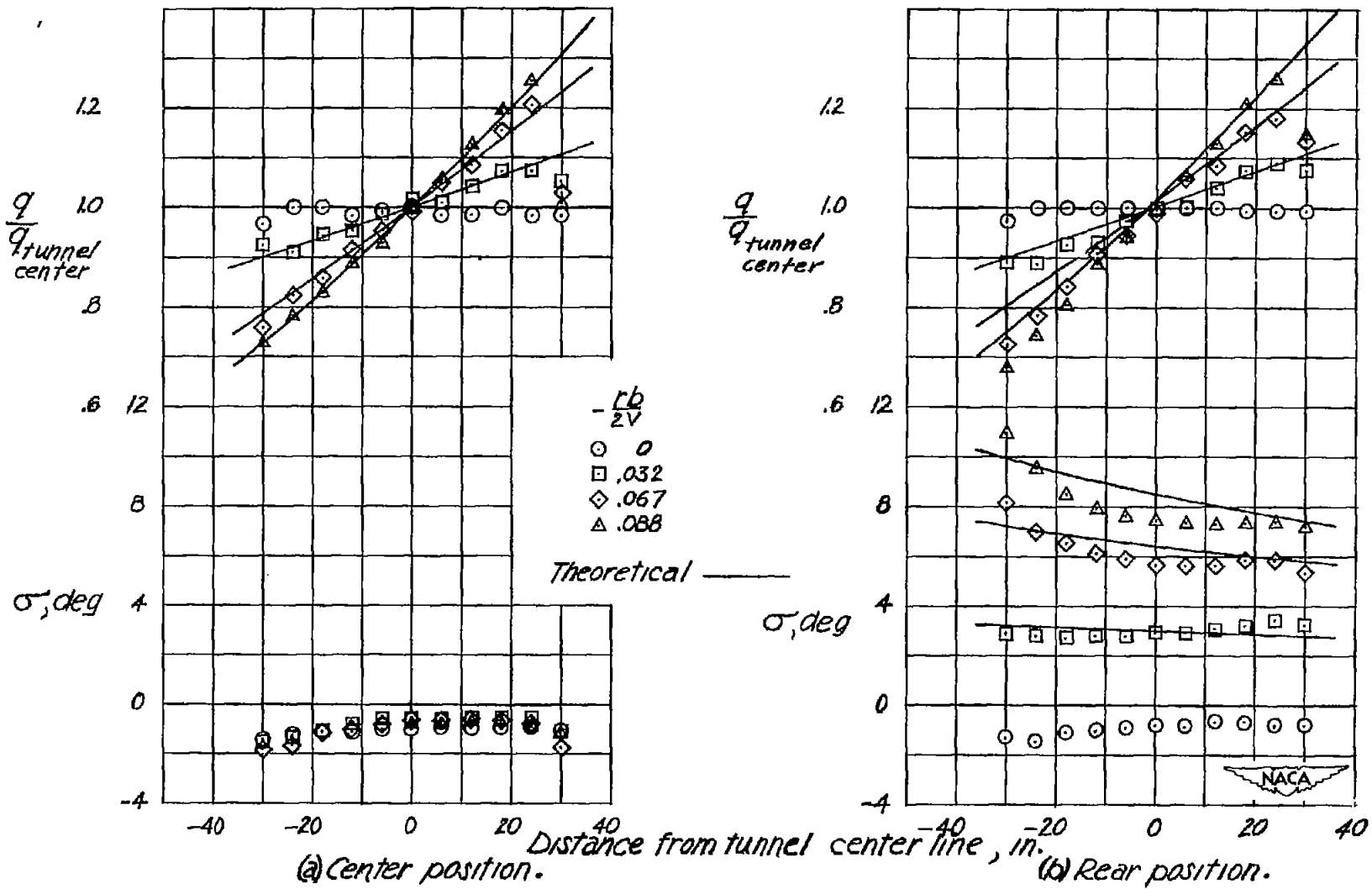


Figure 4.- Variation across test section of dynamic pressure and angularity of air stream in yaw for four flow curvatures.

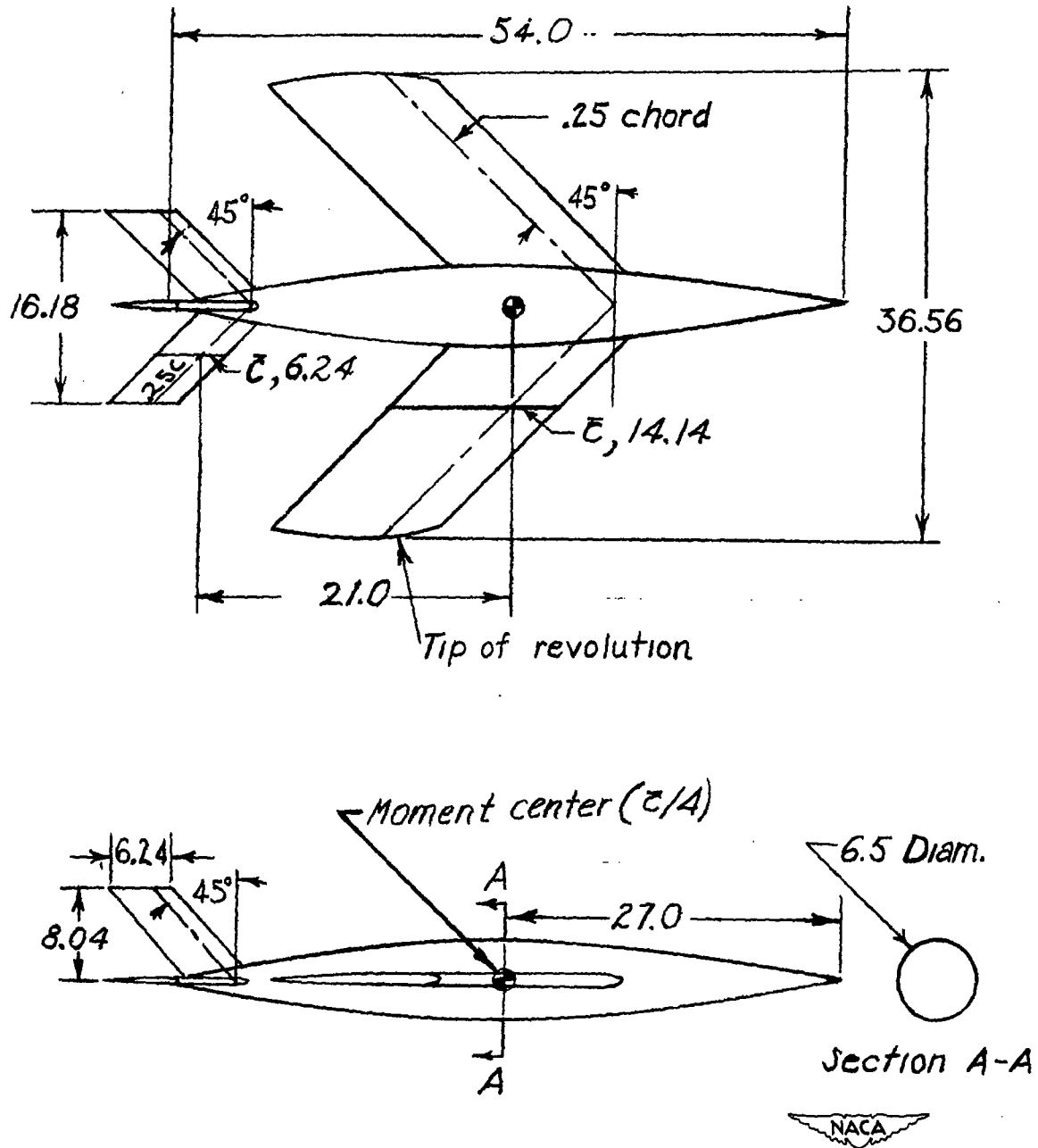


Figure 5.- Geometric characteristics of model. Wing aspect ratio, 2.61. All dimensions are in inches.

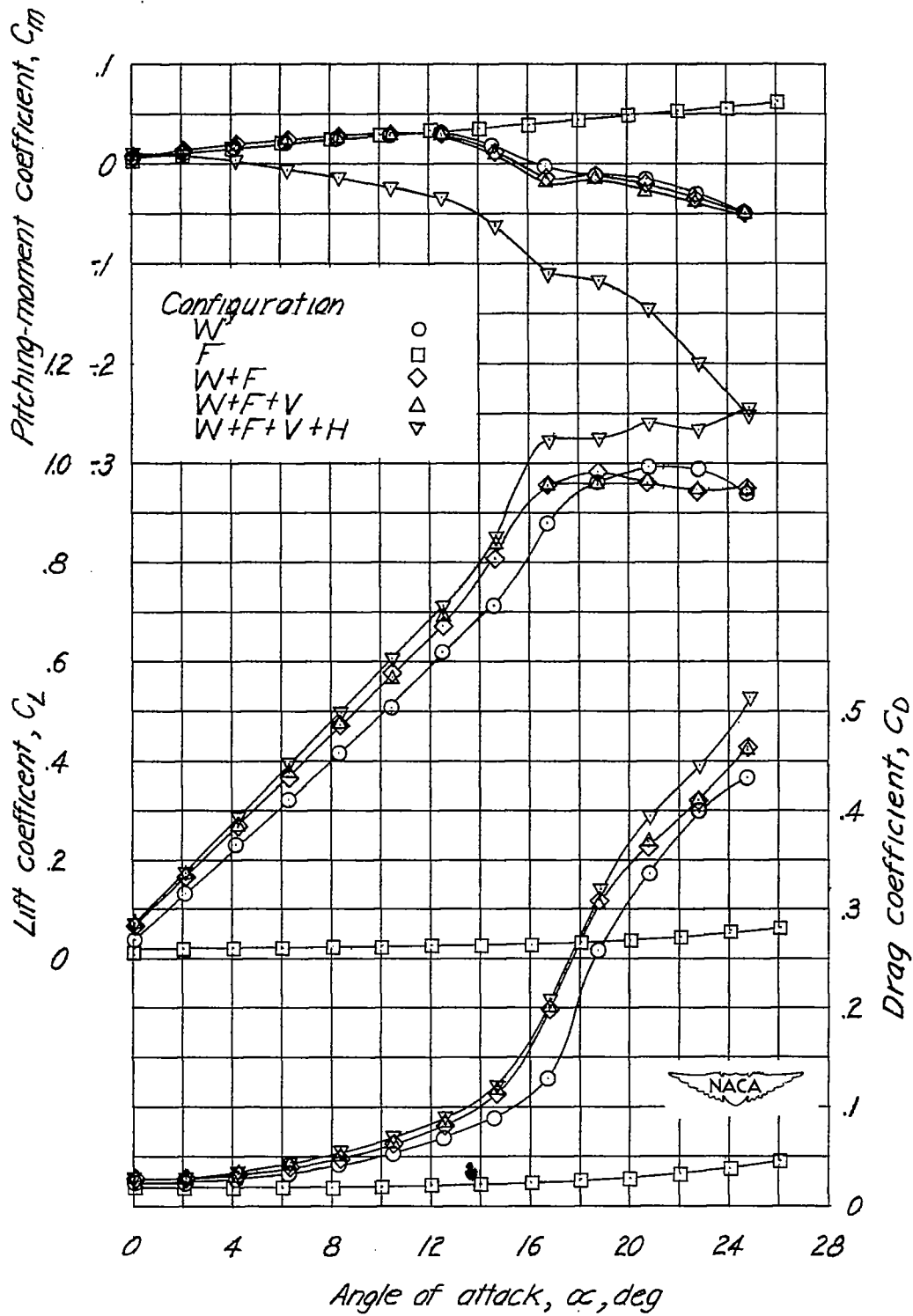


Figure 6.- Variation of lift, drag, and pitching-moment coefficients with angle of attack for all model configurations. $\psi = 0^\circ$; $R = 1.40 \times 10^6$.

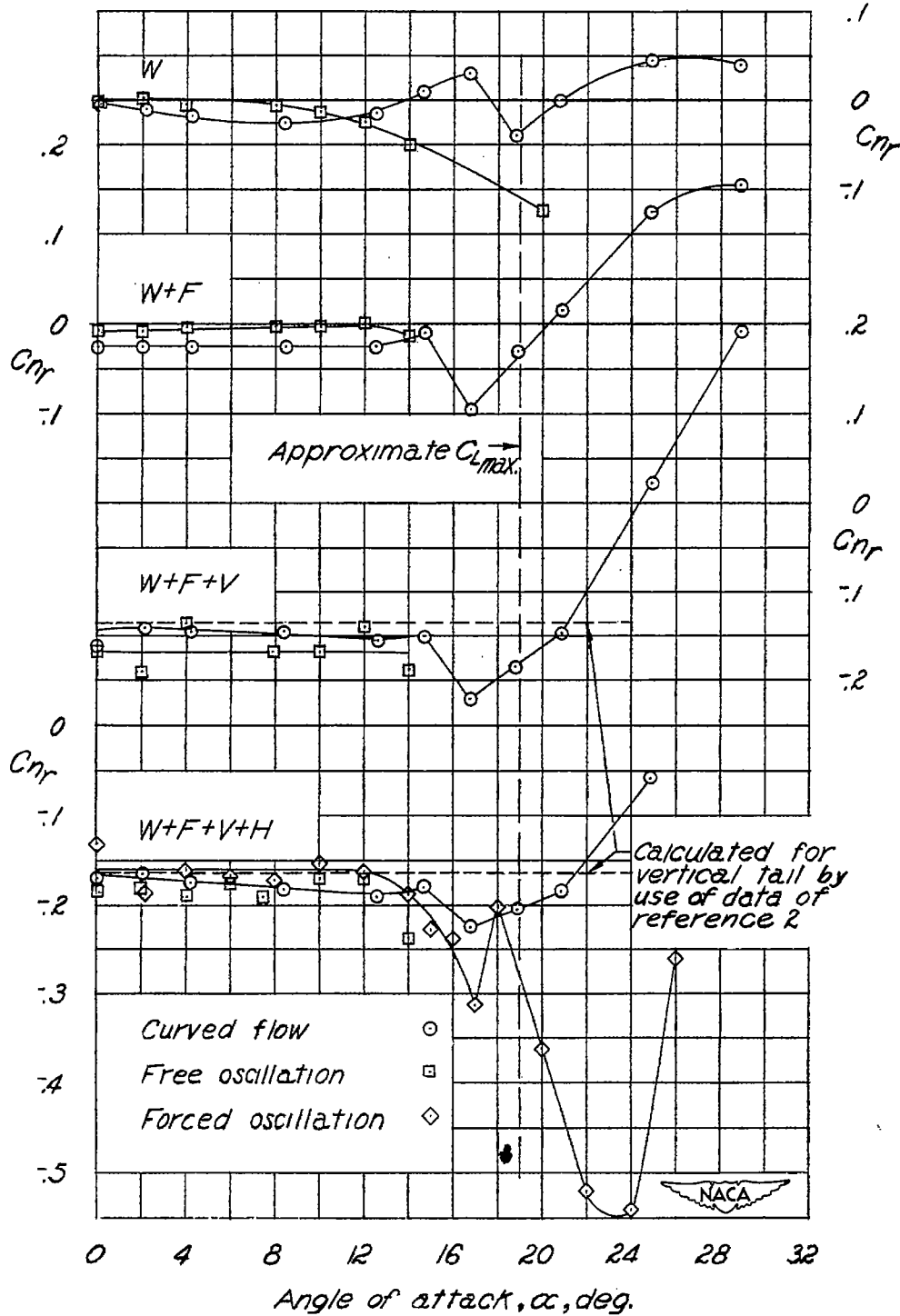


Figure 7.- Comparison of values of C_{nr} obtained by curved-flow, free-oscillation, and forced-oscillation techniques. $R = 1.07 \times 10^6$.

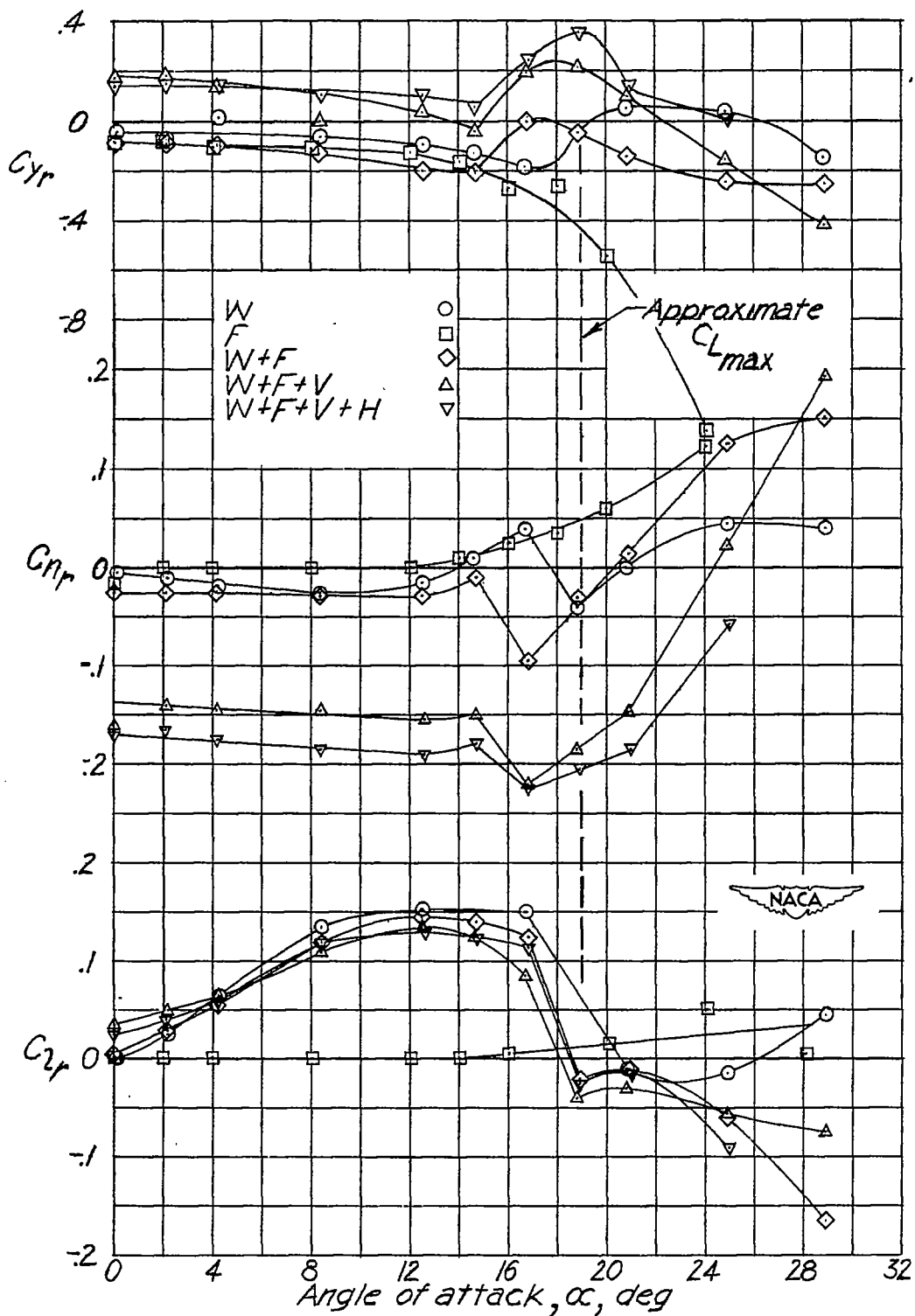


Figure 8.- Variation of C_{l_r} , C_{n_r} , and C_{Y_r} with angle of attack for all model configurations. Curved-flow technique. $R = 1.07 \times 10^6$.